Limnol. Oceanogr., 49(3), 2004, 809–820

Stream denitrification and total nitrate uptake rates measured using a field ^{15}N tracer addition approach

Patrick J. Mulholland[1]
Environmental Sciences Division, Oak Ridge National Laboratory, P.O. Box 2008, Oak Ridge, Tennessee 37831-6036

H. Maurice Valett, Jackson R. Webster, and Steven A. Thomas[2]
Department of Biology, Virginia Tech, Blacksburg, Virginia 24061

Lee W. Cooper
Department of Ecology and Evolutionary Biology, University of Tennessee, Knoxville, Tennessee 37996

Stephen K. Hamilton
W.K. Kellogg Biological Station, Michigan State University, Hickory Corners, Michigan 49060-9516

Bruce J. Peterson
Ecosystems Center, Marine Biological Laboratory, Woods Hole, Massachusetts 02543

Abstract

We measured denitrification and total nitrate uptake rates in a small stream (East Fork of Walker Branch in eastern Tennessee) using a new field ^{15}N tracer addition and modeling approach that quantifies these rates for entire stream reaches. The field experiment consisted of an 8-h addition of 99 atom% $K^{15}NO_3$ and a conservative solute tracer. Two ^{15}N tracer addition experiments were performed on consecutive days, the first under ambient NO_3^- concentrations (23 μg N L^{-1}) and the second with a NO_3^- addition of approximately 500 μg N L^{-1}. We fit first-order NO_3^- uptake and two-box denitrification models to the longitudinal measurements of tracer ^{15}N in dissolved NO_3^-, N_2, and N_2O in stream water to determine rates. Total NO_3^- uptake rates were 0.028 m^{-1} (0.32 μg N m^{-2} s^{-1}) and 0.01 m^{-1} (1.6 μg N m^{-2} s^{-1}) under ambient NO_3^- and with NO_3^- addition, respectively. Denitrification rates were 0.0046 m^{-1} (uncertainty range of 0.002 to 0.008 m^{-1}) and 9×10^{-5} m^{-1} (uncertainty range of 3×10^{-5} to 21×10^{-5} m^{-1}) under ambient NO_3^- and with NO_3^- addition, respectively. Denitrification resulted almost exclusively in N_2 production (>99%) and comprised about 16% (±10%) of total NO_3^- uptake rate under ambient NO_3^- concentrations and about 1% (±1%) of total NO_3 uptake rate with NO_3^- addition. Denitrification rate expressed on a mass flux basis was about 12 μmol m^{-2} h^{-1} under ambient NO_3^- concentrations, a value within the range reported for other streams with low NO_3^- concentrations.

Humans have greatly altered the nitrogen (N) cycle in recent decades, more than doubling the inputs of fixed N to the biosphere (Vitousek et al. 1997). The increased inputs have led to increased hydrologic export of N from landscapes and consequent large increases in the inputs of N, primarily as nitrate–nitrogen (NO_3^--N), via rivers to estuaries and coastal oceans (Howarth et al. 1996; Jordan and Weller 1996). The increases in N loading to streams and rivers have accelerated rates of eutrophication and the development of extensive areas of anoxia and may be linked to harmful algal blooms in a number of coastal ecosystems (Turner and Rabalais 1994; Nixon et al. 1996; Glasgow and Burkholder 2000).

Regional budgets have shown that only 20% to 30% of the N added to the land by humans is exported to the ocean (Howarth et al. 1996; Boyer et al. 2002), indicating that substantial N sinks exist between the land where N is applied and the oceans receiving N loads. In a recent study of the Mississippi River drainage basin, Alexander et al. (2000) showed that rivers were substantial sinks for N originating from terrestrial runoff. Alexander and colleagues found that N retention was inversely related to river size, with retention rates declining exponentially with increasing river depth. Seitzinger et al. (2002) reported that 37% to 78% of the N

[1] Corresponding author (mulhollandpj@ornl.gov).
[2] Present address: Department of Ecology and Evolutionary Biology, Cornell University, Corson Hall, Ithaca, New York 14853-2701.

Acknowledgments

We thank Jeff Houser, Ramie Wilkerson, and Erica Lewis for their help in the field and laboratory; Suzanne Thomas for analysis of ^{15}N samples at the Marine Biological Lab; and Melody Bernot and Jennifer Tank for kindly providing the gas sampling vials. We also appreciate advice on sampling and sample analysis from Jennifer Tank and Melody Bernot. We thank David Harris, Stable Isotope Laboratory, University of California, Davis, for performing most of the ^{15}N analysis. We benefited greatly from discussions with Jim McClelland on transformations of the isotope data and with Wil Wollheim on model development. We also thank two anonymous reviewers for their constructive comments on an earlier version of the manuscript. This work was supported by grants from the U.S. National Science Foundation (DEB-9815868 and DEB-0111410).

inputs to rivers were removed during transport through river networks based on application of a regression model to 16 rivers in the northeastern United States. In contrast to the findings of Alexander et al. (2000), however, Seitzinger et al. (2002) pointed to the importance of larger rivers, suggesting that about one-half of basin-scale N retention occurred in higher order (i.e., ≥fifth) systems.

In an experimental study using $^{15}NH_4$ additions to 12 streams representing multiple biomes, Peterson et al. (2001) reported that the average distance traveled by an ammonium ion before being removed from stream water (defined as the uptake length, S_w) was strongly related to stream discharge, with longer values of S_w (i.e., lower uptake efficiencies) in larger streams. Using a model based on their experimental results, Peterson and colleagues showed that N uptake could reduce inorganic N concentrations by about two-thirds over a 1-km reach of headwater stream with the model most sensitive to nitrate uptake rate.

Although there are a number of processes that remove inorganic N from water, including assimilation by plants and microbes, sorption to sediments, deposition of particulate organic N, and denitrification, it is primarily denitrification that results in permanent loss because the other processes represent primarily internal processes of transformation or relocation. Rates of denitrification in streams and rivers have been measured almost exclusively using the acetylene block technique on sediment cores or slurries returned to the laboratory or in cores or chambers incubated in situ. Studies using this technique have generally shown that denitrification rates are highly variable in space and time. Variation in denitrification rates has been shown to be related primarily to redox status and secondarily to nitrate concentrations and/or the availability of labile organic carbon (Holmes et al. 1996; Duff et al. 1996; Kemp and Dodds 2002). However, the acetylene block technique involves substantial handling of sediments if performed in the laboratory or modification of hydraulic conditions if conducted in field chambers. Thus, this technique may not provide accurate measures of denitrification rates for entire stream ecosystems.

In the past decade, ^{15}N techniques have been developed for determining denitrification rates in aquatic sediments (Nielsen 1992; Rysgaard et al. 1993). These techniques avoid the artifacts associated with the use of acetylene, but past applications still involved use of chambers or cores to isolate sediments and overlying water. Chambers are often problematic to install in streams with coarse or mixed substrata. In addition, there is considerable work on stream biogeochemistry emphasizing the importance of hydrologic exchange between surface and shallow subsurface water (Boulton et al. 1998; Jones and Mulholland 2000), and chamber installation may alter the flow of water through streambed sediments and change the environmental conditions to which denitrification is highly sensitive. Given the recognized potential for stream ecosystems to act as points of substantial N retention along the continuum from land to the ocean, it is important to accurately quantify denitrification rates in streams.

We have developed a field ^{15}N tracer addition approach to quantify denitrification and total nitrate uptake rates for entire stream reaches without physical or chemical perturbation. In this paper, we report the results of an initial set of experimental $^{15}NO_3^-$ additions to determine denitrification and total NO_3^- uptake rates in the East Fork of Walker Branch, a small forested stream in eastern Tennessee. We show that the production of N_2 via denitrification was a small but significant fraction of the total NO_3^- uptake rate even under low nitrate concentrations. However, the production rate of N_2O was quite low and not of significance with respect to the N budget of this stream.

Materials and methods

Study site—The study was conducted in the East Fork of Walker Branch, a first-order stream draining a 59.1-ha deciduous forest catchment in the Ridge and Valley region of eastern Tennessee (35°58′N, 84°17′W). Mean annual precipitation is about 140 cm, and mean annual temperature is about 14.5°C. The catchment is underlain by several layers of siliceous dolomite, and stream water is slightly basic. The stream originates in a headwater spring approximately 100 m above the study reach, and the stream bottom is comprised primarily of cobble, gravel, and fine-grained organic-rich sediments. The average gradient of this stream is quite low (approximately 0.02 m m^{-1}).

The experiments were conducted on 2–3 October 2002 when discharge was low and stable. Although nutrient concentrations are low year-round (<0.1 mg N L^{-1} and <0.01 mg P L^{-1} of inorganic N and P), they are highest at this time of year just prior to substantial leaf-fall inputs, which peak in early November. Previous studies during summer and autumn have indicated that the hydrologic transient storage zone (presumed to be primarily the hyporheic zone) was 0.5 to 1.0 times the size of the surface zone (i.e., $A_S:A$ ratio of 0.5–1.0). Previous measurements of denitrification using the acetylene block technique on sediments returned to the laboratory indicated low to moderate activity (mean rate of 78 ng N_2O g ash-free dry $mass^{-1}$ h^{-1}) limited primarily by nitrate concentrations (Martin et al. 2001).

Experimental procedures—We conducted 8- to 9-h continuous additions of 99% ^{15}N-enriched KNO_3 to the stream on successive days, with the first beginning about 1000 h on 2 October 2002 (day 1) and the second about 0830 h on 3 October 2002 (day 2). The day 1 experiment was conducted under ambient stream NO_3^- concentrations, whereas the day 2 experiment involved addition of unlabeled KNO_3 intended to increase streamwater NO_3^- by about 0.5 mg N L^{-1}. Addition of $K^{15}NO_3$ increased the $^{15}N:^{14}N$ ratio of streamwater NO_3^- by about 40 times relative to the ambient ratio in both experiments. The injection solution consisted of $K^{15}NO_3$ (0.9 g and 6.2 g 99% ^{15}N-enriched KNO_3 on day 1 and 2, respectively) added to 15 liters of deionized water together with NaCl (200 g on each date) to provide a conservative solute tracer for each experiment. On day 2, 2.5 g of unlabeled KNO_3 were also added to the 15-liter injection solution. The $K^{15}NO_3$ addition resulted in a small increase in the streamwater NO_3^- concentration—approximately 15% above the ambient concentration (23 μg N L^{-1}) on day 1 and 15% above the target enrichment on day 2.

The injection solution was pumped using a fluid metering

pump (FMI Inc.) into the stream at approximately 25 ml min^{-1} over the duration of each experiment. The injection site was immediately above a constricted, turbulent section of stream that afforded complete mixing of the injected solution prior to the first sampling station 7 m downstream. Samples of water for isotopic and chemical analysis were collected at an upstream station (5 m upstream from the injection site) and at four to seven stations downstream from the injection location 7 to 8 h after the injection began.

Water temperature and samples for $^{15}NO_3^-$, chloride (Cl^-), NO_3^-, and ammonium (NH_4^+) were collected from the upstream and four downstream stations ranging in distance from 7 to 87 m from the ^{15}N injection location. Single samples were collected from the second and fourth stations and replicate samples from the first and third stations downstream from the ^{15}N injection. All samples were returned to the laboratory and filtered through Whatman GFF glass-fiber filters (nominal pore size = 0.7 μm) within 2 h of collection. Spikes of unlabeled KNO_3 of approximately 200 μg N L^{-1} (day 1) and 5 mg N L^{-1} (day 2) were added to 1-liter samples for ^{15}N-NO_3^- analysis to reduce ^{15}N : ^{14}N ratios to the ideal working range for mass-spectrometric measurement. Identical spikes were also added to 1-liter samples of deionized water to calculate N recovery and determine the ^{15}N : ^{14}N ratio of the NO_3^- spike. Cl was determined by ion chromatography, NO_3^- by automated Cu-Cd reduction followed by azo dye colorimetry, and NH_4 by automated phenate colorimetry, the latter two analyses on a Bran Luebbe auto analyzer 3. The NO_3^- measurement is actually $NO_3^- + NO_2^-$, but NO_2^- is assumed to be negligible in this well-oxygenated stream (Mulholland 1992).

Processing of samples for ^{15}N-NO_3^- analysis was modified from the method of Sigman et al. (1997). Samples ranging in volume from 0.05 to 1 liter (depending on NO_3^- concentration) were added to glass flasks together with 5 g of NaCl and 3 g of MgO. For small samples (high NO_3^- concentrations), deionized water was added to bring the initial sample volume to 200 ml. The samples were then brought to a gentle boil on a hot plate until the volume was reduced to about 100 ml, thereby concentrating $^{15}NO_3^-$ and removing NH_3 produced from NH_4^+ under alkaline conditions. The concentrated samples were then cooled, transferred to 250-ml high density polyethylene bottles, and refrigerated until further processing. The $^{15}NO_3^-$ in the concentrated samples was captured using a reduction/diffusion/sorption procedure as follows. An additional 0.5 g of MgO and 3 g of Devarda's alloy was added to each sample to reduce all NO_3^- to NH_4^+. A filter packet consisting of a precombusted 1-cm glass-fiber filter (Whatman GFD) to which 25 μl of 2.5 mol L^{-1} $KHSO_4$ was added to absorb NH_3 was sealed between two Teflon filters (Millipore white nitex LCWP 25-mm diameter, 10-μm pore size). The filter packet was then immediately placed on the surface of the concentrated sample, Parafilm® placed over the bottle mouth, and the bottle tightly capped. Samples were then heated to 60°C for 2 d and shaken at room temperature for an additional 7 d to allow reduction of NO_3^- to NH_4^+, conversion of NH_4^+ to NH_3, diffusion of NH_3 into the sample headspace, and absorption of NH_3 onto the GFD filter. The filter packets were then removed from the sample bottles and dried in a desiccator for 2 d, after which the Teflon filter packet was opened and the GFD filter removed. The GFD filters with absorbed NH_3 were encapsulated in tins, placed in a 96-well titer plate with each well capped, and sent to the stable isotope laboratory at the University of California at Davis (http://stableisotopefacility.ucdavis.edu) for ^{15}N : ^{14}N ratio analysis by mass spectrometry using a Europa Integra continuous flow isotope ratio mass spectrometer (IRMS) coupled to an in-line elemental analyzer for automated sample combustion.

Samples for ^{15}N analysis of dissolved N_2 and N_2O were collected from the upstream station and seven stations ranging from 7 to 87 m downstream from the ^{15}N injection site. At each station, 50 ml of stream water was collected in 60-ml plastic syringes (Becton-Dickinson 60-ml disposable syringes) and all visible air bubbles were expelled. The samples were kept submerged in stream water after collection until the headspace equilibration was performed (within 30 min). Replicate samples were collected from the first four stations downstream from the ^{15}N injection, while single samples were collected from the other stations. After all samples were collected, needles were affixed to the syringes, 5 ml of water expelled (leaving a sample volume of 45 ml), and 15 ml of high purity helium was added to each syringe from a gas bag submerged in stream water to minimize air contamination. Samples were then shaken gently for 15 min while submerged in stream water to allow for equilibration of dissolved gases between water and the He headspace. Approximately 13 ml of headspace gas was then injected into preevacuated 12-ml exetainers (Labco, evacuated/labeled type 3 screw-cap with septa) while the syringe and exetainer were submerged in a large bucket filled with stream water. A bead of silicone sealant was placed over the exetainer septa and the samples shipped to the stable isotope laboratory at the University of California, Davis, for ^{15}N : ^{14}N ratio analysis by mass spectrometry using a Europa Hydra Model 20/20 continuous flow IRMS. These analyses were performed within 3 weeks of sample collection.

Six additional samples for ^{15}N analysis of N_2 were collected during the NO_3^- addition experiment on day 2 (three samples from the upstream station and three samples from a station 28 m downstream from the $^{15}NO_3^-$ injection). Water samples were collected in evacuated 150-ml glass bulbs until approximately one-half full by submersing the bulb in the stream and opening the stopcock. The glass bulbs contained 1 ml of a saturated HgCl solution to prevent the microbial transformation of N after sample collection. On a vacuum line, the headspace gas was cryogenically separated to remove water vapor and CO_2, then collected in a Pyrex tube containing silica gel and copper oxide. Once the tube was sealed, it was then combusted to remove oxygen and analyzed on a Finnigan MAT Delta S mass spectrometer for ^{15}N : ^{14}N ratios at the Marine Biological Laboratory, Woods Hole, Massachusetts. Nitrogen : argon ratios were also recorded from the mass-spectrometer analysis and used to check for atmospheric N_2 contamination of the samples. Samples were analyzed within 2 months of collection.

Measurements of ^{15}N : ^{14}N ratio are expressed as $\delta^{15}N$ values (units of ‰) according to the following equation:

$$\delta^{15}\mathrm{N} = \left[\left(\frac{R_{\mathrm{SAMPLE}}}{R_{\mathrm{STANDARD}}}\right) - 1\right] \times 1{,}000 \qquad (1)$$

where R_{sample} is the $^{15}N:^{14}N$ ratio in the sample and $R_{standard}$ is the $^{15}N:^{14}N$ ratio in atmospheric N_2 ($R_{standard} = 0.0036765$).

We measured air–water gas exchange rates using a propane/conservative tracer injection method (sensu Marzolf et al. 1994) the day following the $^{15}NO_3^-$ additions (day 3) under similar discharge rates. Propane and a conservative tracer (100 g L^{-1} NaCl solution) were injected simultaneously at constant rates. Propane was injected using a large bubble diffuser and NaCl using the same pump used for the $^{15}NO_3^-$ injection. Water samples for dissolved propane were collected at two stations (7 and 43 m) downstream from the injection site approximately 3 h after the injection began. Six 45-ml water samples were collected in 60-ml polyethylene syringes at each station, and 10 ml of headspace air was added to each syringe. Samples were immediately returned to the laboratory, shaken gently for 2 h, and a subsample of the headspace was removed and analyzed for propane by gas chromatography using a flame ionization detector. Propane readings were normalized to the increase in conservative tracer concentration at each station determined as the increase in specific conductance using a YSI Model 30 field conductivity meter (Yellow Springs Instrument Co.) to account for dilution due to groundwater input. The gas exchange rate for propane (k_P, m^{-1}) was calculated as the slope of a regression of the natural log of conservative tracer-normalized propane readings versus distance.

Gas exchange rates of N_2 and N_2O were calculated from the measured values of k_P using the relative values of their Schmidt numbers (Sc). Gas transfer rates of two gases, denoted as k_A and k_B, can be related through the Schmidt number Sc, defined as the kinematic viscosity of the water divided by the diffusion coefficient of the gas (MacIntyre et al. 1995):

$$k_A = k_B\left(\frac{\mathrm{Sc}_A}{\mathrm{Sc}_B}\right)^x \qquad (2)$$

where x is the Schmidt number dependence that ranges between $-2/3$ for smooth water surfaces and $-1/2$ for rough surfaces (Jähne et al. 1987). For streams, the value of x is likely to be about $-1/2$ (Wanninkhof et al. 1990; MacIntyre et al. 1995). Because at a given temperature the kinematic viscosity of water is the same in the numerator and denominator of Eq. 2, we can substitute the diffusion coefficients D_A and D_B for the Schmidt numbers. Using Eq. 2 and data from table A1 in Wanninkhof (1992) based on N_2 and N_2O diffusion coefficients determined by Jähne et al. (1987) and a propane diffusion coefficient determined by Wise and Houghton (1966), we calculated that the air–water exchange rates of N_2 and N_2O were 0.98 and 0.96 times the measured values of k_P. These relationships appear to be essentially independent of temperature over the range experienced by temperate streams (Rainwater and Holley 1984).

Calculations of tracer ^{15}N flux—Tracer ^{15}N flux was calculated from the measured $\delta^{15}N$ values by first converting all $\delta^{15}N$ values to $^{15}N/(^{15}N + {}^{14}N)$ ratios using the following equation:

$$\frac{{}^{15}\mathrm{N}}{{}^{15}\mathrm{N} + {}^{14}\mathrm{N}} = \frac{\left(\frac{\delta^{15}\mathrm{N}}{1{,}000} + 1\right) \times 0.0036765}{1 + \left[\left(\frac{\delta^{15}\mathrm{N}}{1{,}000} + 1\right) \times 0.0036765\right]} \qquad (3)$$

Hereafter we will call $^{15}N/(^{15}N + {}^{14}N)$ the isotopic mole fraction of ^{15}N (MF).

We then corrected $^{15}NO_3^-$ MF values for the added nitrate spike using the following equation:

$$\mathrm{MF}_i = \{([\mathrm{NO_3} - \mathrm{N}_i] + [\mathrm{NO_3} - \mathrm{N_{sp}}])(\mathrm{MF_{mi}}) - ([\mathrm{NO_3} - \mathrm{N_{sp}}])(\mathrm{MF_{sp}})\}/[\mathrm{NO_3} - \mathrm{N}_i] \qquad (4)$$

where $[NO_3\text{-}N_i]$ is the measured nitrate N concentration at station i (μg N L^{-1}), $[NO_3\text{-}N_{sp}]$ is the nitrate N concentration increase resulting from the nitrate spike (μg N L^{-1}, same for all stations), MF_{mi} is the MF at station i calculated from the measured $\delta^{15}N$ values on spiked samples from station i using Eq. 3, MF_{sp} is the MF of the nitrate spike calculated from the measured $\delta^{15}N$ values of nitrate in the deionized water samples that also received the nitrate spike, and MF_i is the true MF of nitrate at station i.

We then computed total $^{15}NO_3^-$ mass flux at each station i ($^{15}N_{flux\ i}$, units of μg s^{-1}) by multiplying MF_i by the streamwater nitrate concentration ($[NO_3\text{-}N_i]$) and stream discharge (Q_i) at each station i as follows:

$$^{15}\mathrm{N}_{\mathrm{flux}\ i} = \mathrm{MF}_i \times [\mathrm{NO_3} - \mathrm{N}_i] \times Q_i \qquad (5)$$

Stream discharge at each station (Q_i) was determined from the increase in streamwater Cl^- concentration during the injection as follows:

$$Q_i = ([\mathrm{Cl_{inj}}] \times Q_{\mathrm{pump}})/([\mathrm{Cl}_i] - [\mathrm{Cl}_b]) \qquad (6)$$

where the Cl^- injection rate (mg s^{-1}) was determined as the product of the Cl^- concentration in the injection solution ($[Cl_{inj}]$) and the solution injection rate (Q_{pump}), and the increase in Cl^- concentration at each station i is the difference between [Cl] during the injection ($[Cl_i]$) and the measured Cl^- concentration just prior to the ^{15}N injection (i.e., background concentration, $[Cl_b]$).

Finally, we computed tracer $^{15}NO_3^-$ mass flux at each station i by subtracting background $^{15}NO_3^-$ mass flux from the total $^{15}NO_3^-$ mass flux. Background $^{15}NO_3^-$ mass flux at each station i was calculated using Eq. 5 except that the MF determined for the station upstream from the ^{15}N addition was used instead of the measured value of MF_i.

For $^{15}N_2$ and $^{15}N_2O$ we first corrected the measured headspace $\delta^{15}N$ values for equilibrium isotopic fractionation during the headspace equilibration using the estimated masses of N in the gas and liquid phases of the equilibration system and the following equation:

$$\delta^{15}\mathrm{N}_{\mathrm{fc}} = \delta^{15}\mathrm{N}_m - \varepsilon \qquad (7)$$

where $\delta^{15}N_{fc}$ is the fractionation-corrected $\delta^{15}N$ value, $\delta^{15}N_m$ is the measured $\delta^{15}N$ value, and ε is the isotopic enrichment factor for N_2 (-0.85‰; Klots and Benson 1963) and N_2O

(−0.75‰; Inoue and Mook 1994), respectively. The concentrations of N_2 and N_2O were calculated from N mass values determined in the headspace as part of the mass-spectrometric analysis and corrected for incomplete gas transfer into the headspace using the relative volumes of water and headspace and the Bunsen coefficients for N_2 and N_2O at the temperature and pressure at which the headspace equilibration was performed. MF_i values for each gas were then calculated using Eq. 3 except that $\delta^{15}N_{fc}$ values were used instead of the measured $\delta^{15}N$ values. The fluxes of total ^{15}N in N_2 and N_2O at each station i were calculated from the MF_i values, the N_2 and N_2O concentrations in stream water, and stream discharge using Eq. 5. The stream discharge at each station was determined as described above (Eq. 6) and interpolated for stations at which $^{15}N_2$ and $^{15}N_2O$ samples but no $^{15}NO_3^-$ samples were collected. Finally, fluxes of tracer ^{15}N in N_2 and N_2O at each station i were determined by subtracting the background ^{15}N flux at that station (calculated by Eq. 5 but using the MF determined for the station upstream from the ^{15}N addition rather than MF_i) from the total ^{15}N flux.

Calculation of NO_3^- uptake rate and length—The total uptake rate of NO_3^-, expressed as a fractional uptake rate per unit distance (k_{tot}), was calculated from the regression of ln (tracer $^{15}NO_3^-$ flux) versus distance from the ^{15}N injection for each injection. The inverse of the slope of these regressions is the uptake length of NO_3^- (S_w; Newbold et al. 1981; Stream Solute Workshop 1990). The total NO_3^- uptake rate was also calculated as a mass removal rate from water per unit area (U) using the following equation:

$$U = \frac{F \times k_{tot}}{w} \tag{8}$$

where F is the average flux of NO_3-N in streamwater in the experimental reach (determined as the product of average NO_3-N concentration and average discharge) and w is the average stream wetted width (Newbold et al. 1981). Total NO_3^- uptake rate was also calculated as a mass transfer velocity (V_f) using the following equation (Stream Solute Workshop 1990):

$$V_f = \frac{U}{C} \tag{9}$$

where C is the average stream NO_3^- concentration.

Determination of N_2 and N_2O production rates via denitrification—Production rates of N_2 and N_2O (considered separately) were estimated by fitting a model of N gas production to the longitudinal pattern in the fluxes of tracer ^{15}N as N_2 and N_2O over the study reach. The model simulates N_2 and N_2O production from NO_3^- (k_{den}), air–water exchange (k_2) of N_2 and N_2O, and the assimilative uptake of NO_3^- (k_U) in a 1-m reach of stream (Fig. 1). Change in tracer ^{15}N fluxes with distance x are expressed as follows:

$$\partial {}^{15}NO_3/\partial x = -(k_{den} + k_U){}^{15}NO_3 \tag{10}$$

$$\partial {}^{15}N_{gas}/\partial x = k_{den}{}^{15}NO_3 - k_2{}^{15}N_{gas} \tag{11}$$

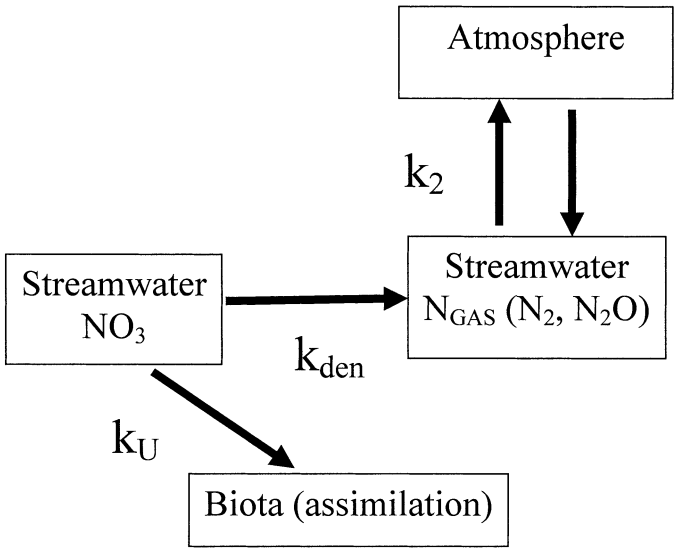

Fig. 1. Model of N_2 and N_2O production from NO_3^- in streams.

where $^{15}NO_3$ is the tracer ^{15}N flux in NO_3^- and $^{15}N_{gas}$ is the tracer ^{15}N flux in N_2 or N_2O. The fractional total uptake rate of NO_3^- (k_{tot}) is the sum of denitrification and assimilatory uptake (i.e., $k_{den} + k_U$). The steady state solutions for $^{15}NO_3$ and $^{15}N_{gas}$ are

$$^{15}NO_3 = (^{15}NO_3)_0 \times [e^{-(k_{den}+k_U)x}] \tag{12}$$

$$^{15}N_{gas} = \left[\frac{k_{den}(^{15}NO_3)_0}{k_2 - k_{den} - k_U}\right] \times [e^{-(k_{den}+k_U)x} - e^{-k_2 x}] \tag{13}$$

where $(^{15}NO_3)_0$ is the tracer $^{15}NO_3$ flux at the injection site ($x = 0$).

We used a least-squares fitting procedure in conjunction with a spreadsheet model of Eq. 13 (using Microsoft Excel optimization tool ''Solver''; Microsoft) to estimate values of k_{den} from the tracer ^{15}N mass flux data for N_2 and N_2O separately ($^{15}N_{gas}$). Values of k_{tot} were determined from the regression of ln (tracer $^{15}NO_3^-$ flux) versus distance as described above. Values of k_2 were determined from the measured rates of propane gas exchange converted to N_2 and N_2O exchange rates using Eq. 2. Denitrification rates were also calculated as NO_3^- mass removal rates per unit area (DN) for N_2 and N_2O production separately using Eq. 8 with k_{den} substituted for k_{tot}.

Figure 2 presents model simulations of tracer $^{15}N_{gas}$ flux for a stream with a NO_3^- uptake length of 50 m, equivalent to a fractional total uptake rate ($k_{tot} = k_U + k_{den}$) of 0.02 m^{-1}, and three different combinations of the gas exchange rate (k_2) and denitrification rate (k_{den}). The tracer $^{15}N_{gas}$ flux curve is hump shaped because of the longitudinal decline in labeled substrate (i.e., tracer $^{15}NO_3^-$) available for denitrification. The maximum tracer $^{15}N_{gas}$ flux is primarily dependent on the value of k_{den} relative to k_2 (higher for high k_{den} relative to k_2). The distance at which maximum tracer $^{15}N_{gas}$ flux occurs is dependent on the value of k_2 relative to k_{tot} (e.g., shorter for high k_2 relative to k_{tot}).

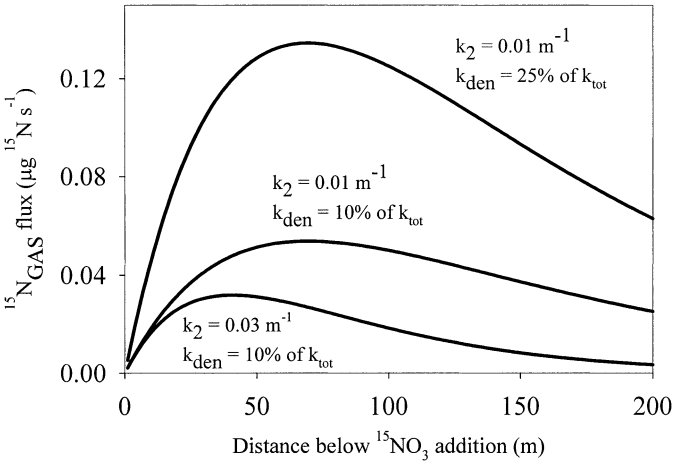

Fig. 2. Simulation of tracer $^{15}N_{gas}$ flux for a stream with a total NO_3^- uptake length of 50 m and fractional total uptake rate ($k_{tot} = k_U + k_{den}$) of 0.02 m^{-1}, tracer $^{15}NO_3^-$ flux in stream water at the injection location of 1 μg ^{15}N s^{-1}, and three different scenarios for the gas exchange rate (k_2) and the denitrification rate (k_{den}, i.e., the N_{gas} production rate).

Results

Physical and chemical conditions in the East Fork of Walker Branch during the ^{15}N experiments are given in Table 1. Weather conditions were generally clear, and stream discharge was stable, although it increased over the length of the study reach by about a factor of 2 due to groundwater inflow. NO_3^- concentrations declined over the study reach, from 27 to 13 μg N L^{-1} during the ambient NO_3^- experiment and from about 580 to 166 μg N L^{-1} during the NO_3^- addition, indicating substantial net uptake of NO_3^- in this stream. Concentrations of NH_4^+ were relatively low, and NO_3^- was the dominant component of dissolved inorganic N (Table 1).

^{15}N-NO_3^- MF values during the experiments were considerably higher downstream compared with upstream from the ^{15}N additions and declined sharply over the experimental reach (Fig. 3A,B). Total uptake rates of NO_3^- from water, determined from the longitudinal decline in tracer $^{15}NO_3^-$ flux and expressed as a fractional rate per unit distance (k_{tot}) and as a mass transfer velocity (V_f) declined about threefold when NO_3^- concentrations were increased compared with ambient conditions (Fig. 3C,D; Table 2). This resulted in a threefold increase in NO_3^- uptake length (S_W) with NO_3^- addition. However, the total mass removal rate of NO_3^- from water per unit area (U) increased more than fivefold with NO_3^- addition (Table 2), indicating that total NO_3^- uptake from stream water was stimulated by NO_3^- addition.

There was evidence that the $^{15}N_2$ samples were contaminated with atmospheric N_2. The headspace N_2 mass determined for samples collected during the ambient experiment ranged from 100 to 160 μmol, with the exception of one sample with 220 μmol. The N_2 mass determined for samples during the NO_3^- addition experiment ranged from 180 to 220 μmol, with the exception of two samples with 290 and 320 μmol. The N_2 mass expected in our headspace samples for water in equilibrium with the atmosphere is about 20 μmol; thus, our samples contained 5 to 16 times more N_2 than expected. Because it is unlikely that the stream water was more than a few percent supersaturated with N_2, the high N_2 mass values measured were probably the result of inadvertent contamination by atmospheric N_2, possibly introduced during sampling, sample equilibration, or storage of the exetainers. The excess N_2 would dilute the tracer ^{15}N in the sample and lead to smaller background-corrected MF values. The three samples with the highest levels of air contamination relative to the others for that experiment were not included in subsequent analyses. Although important for N_2, these levels of air contamination are relatively unimportant for N_2O, which exists at only trace levels in air.

Values of ^{15}N MF for N_2 and N_2O generally exhibited hump-shaped distributions with distance (Fig. 4A,B). ^{15}N MF values for N_2O were considerably higher and the spatial distribution of the data more consistent than for N_2, a result of the much lower mass of N_2O (ranging from 0.13 to 0.20 nmol) that permitted detection of a much larger tracer ^{15}N signal in our samples. There was little difference in the ^{15}N MF values for N_2 between experiments; however, the MF values for N_2O were considerably higher during the NO_3^- addition than during the ambient NO_3^- experiment.

Measurements of ^{15}N-N_2 in the evacuated glass bulb samples collected during the NO_3^- addition experiment at the upstream and 28-m stations indicated substantial enrichment

Table 1. Conditions during the ^{15}N tracer addition experiments in the East Fork of Walker Branch. Values for discharge, water temperature, and N and Cl concentrations are averages for the study reach (mean of values measured at 7, 28, 57, and 87 m) during the experiments (range is given in parentheses). Average wetted width is the mean of measurements made at 1-m intervals along the study reach (range in parentheses). The values for NO_3^- concentration include the effect of a small increase in concentration due to the $^{15}NO_3^-$ addition (about 15%). The ambient experiment values given below are typical for this stream during this time of year.

Parameter	Ambient NO_3^- experiment (2 October 2002)	NO_3^- addition experiment (3 October 2003)
Discharge (L s^{-1})	0.4 (0.3–0.7)	0.4 (0.3–0.6)
Average wetted width (m)	0.92 (0.6–2.0)	0.92 (0.6–2.0)
Average water velocity (cm s^{-1})	1.5	1.5
Water temperature (°C)	20.0 (19.5–20.5)	20.1 (19.5–20.7)
NO_3^- concentration (μg N L^{-1})	26 (19.6–39.8)	380 (166–580)
NH_4^+ concentration (μg N L^{-1})	4 (1.8–8)	5 (3.8–7.8)
Cl^- concentration (mg L^{-1})	1.1 (1.09–1.15)	1.1 (1.09–1.15)

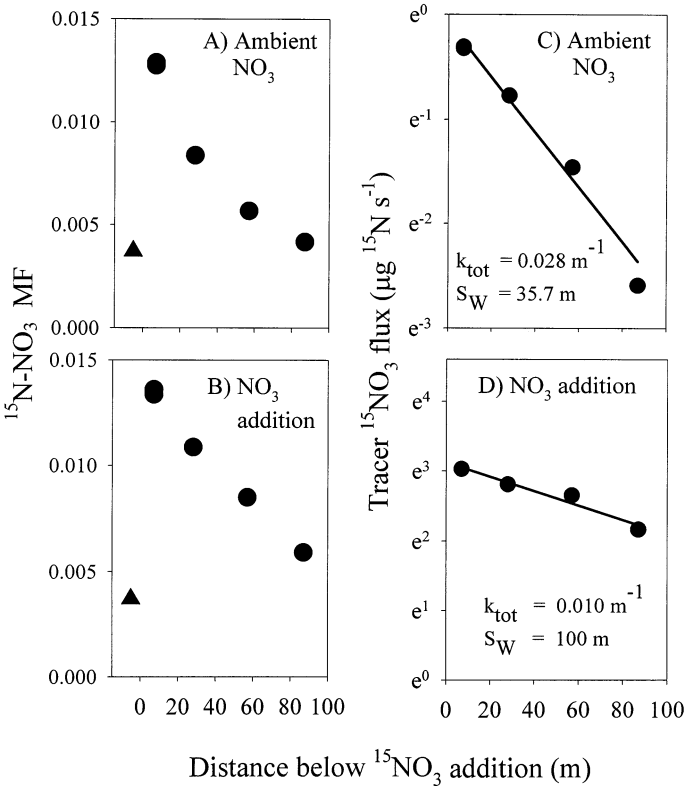

Fig. 3. $^{15}N\text{-}NO_3^-$ MF values for the upstream station (−5 m, triangles) and four stations downstream (circles) from the ^{15}N addition location for the (A) ambient NO_3^- and (B) NO_3^- addition experiments. MF values of replicate samples at 7 and 57 m were within 0.0002 of each other and appear as one point on these plots. Also shown are plots of ln (tracer $^{15}NO_3^-$ flux) versus distance downstream from the $^{15}NO_3^-$ addition for the (C) ambient and (D) NO_3^- addition experiments. The slopes of the regression lines are the total fractional NO_3^- uptake rates (k_{tot}) and the inverse of the slopes are the uptake lengths for NO_3^- (S_w). Fluxes calculated from replicate samples collected from the 7- and 57-m stations during both experiments differed by <3%, and the mean values at these stations were used in the regressions.

of tracer ^{15}N downstream from the ^{15}N addition. The mean $^{15}N\text{-}N_2$ MF at the 28-m station was 3.678×10^{-3} (SD = 0.002×10^{-3}, $n = 3$), significantly higher than the mean $^{15}N\text{-}N_2$ MF at the upstream station (3.666×10^{-3}, SD = 0.001×10^{-3}, $n = 3$, $p = 0.004$). In addition, the mean $^{15}N\text{-}N_2$ MF for the bulb samples at 28 m was about 0.006 higher than the MF determined using the headspace equilibration and exetainer gas storage method at the same station and time. Based on N_2/Ar ratios measured in the bulb samples, there appeared to be little if any contamination of these samples by atmospheric N_2 (Suzanne Thomas, Marine Biological Laboratory, unpubl. data). Thus, the higher $^{15}N\text{-}N_2$ MF for the bulb sample compared with the $^{15}N\text{-}N_2$ MF for the exetainer sample appears to be the result of dilution of tracer ^{15}N due to atmospheric N_2 contamination in the latter.

The air–water exchange rate of propane was 0.056 m^{-1} (95% CI: 0.048 to 0.064 m^{-1}). This measurement was for the reach from 7 to 43 m and was similar to a propane exchange rate of 0.051 m^{-1} measured for the reach from 7

Table 2. Total NO_3^- uptake rates and denitrification rates (N_2 and N_2O production separately and in total) presented as fractional uptake rates (k), mass flux rates per unit area (U and DN), and mass transfer velocities (V_f). Uptake lengths for NO_3^- (S_w) based on total NO_3^- uptake and denitrification (sum of N_2 and N_2O production rates) are also given.

Parameter	Ambient NO_3^- experiment	NO_3^- addition experiment
Total NO_3^- uptake rates and length		
k_{tot} (m^{-1})	0.028	0.010
S_w (m)	35.7	100
U (μg N m^{-2} s^{-1})	0.32	1.65
V_f (m h^{-1})	0.044	0.016
NO_3^- uptake rates from denitrification		
k_{den} N_2 (m^{-1})	0.0046	8.8×10^{-5}
k_{den} N_2O (m^{-1})	6.8×10^{-6}	3.0×10^{-6}
DN N_2 (μg N m^{-2} s^{-1})	0.045	0.013
DN N_2O (μg N m^{-2} s^{-1})	6.6×10^{-5}	4.2×10^{-4}
V_f N_2 (m h^{-1})	0.0062	1.2×10^{-4}
V_f N_2O (m h^{-1})	9.1×10^{-6}	4.0×10^{-6}
Total denitrification-based NO_3^- uptake rate and length		
k_{den} N_2+N_2O (m^{-1})	0.0046	9.1×10^{-5}
S_w (m)	217	10,989
DN (μg N m^{-2} s^{-1})	0.0451	0.0134
V_f (m h^{-1})	0.00621	1.24×10^{-4}

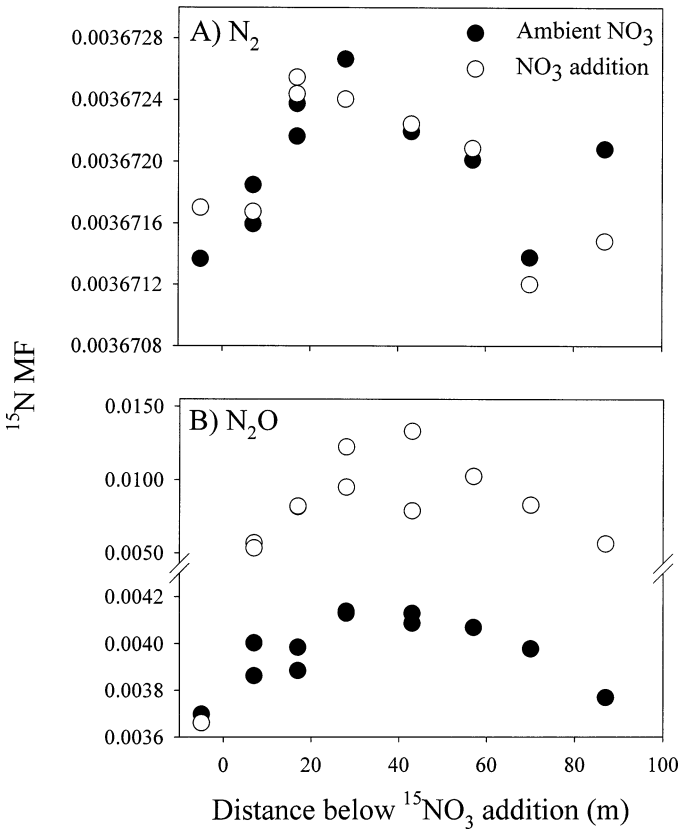

Fig. 4. ^{15}N MF values versus distance below the ^{15}N addition location for (A) N_2 and (B) N_2O. The data points at a distance of −5 m are for samples collected 5 m upstream from the ^{15}N addition and represent background MF values.

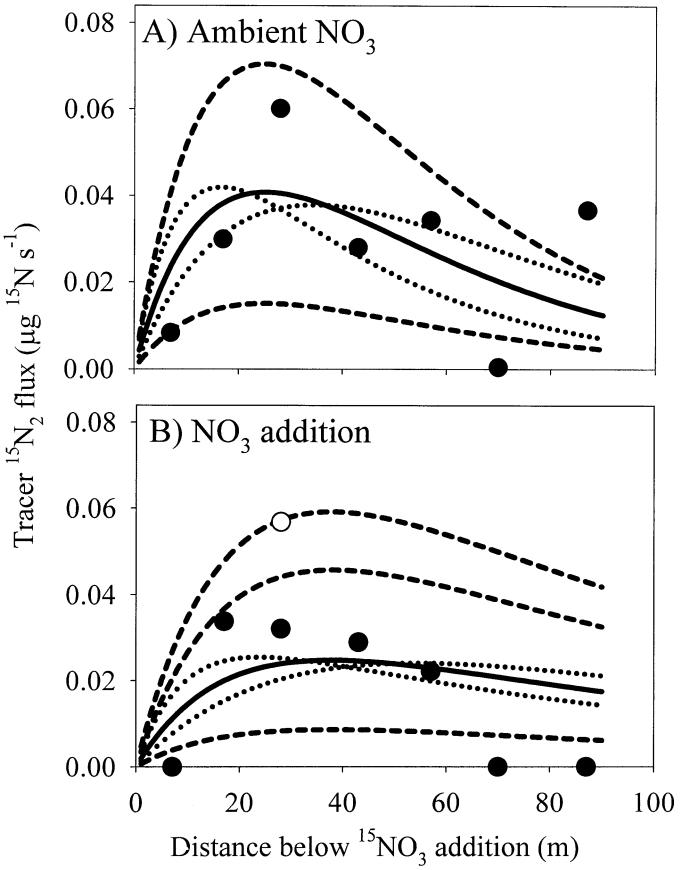

Fig. 5. Measured values of tracer $^{15}N_2$ flux versus distance below the $^{15}NO_3^-$ addition (filled circles) and least-squares fits of the denitrification model (solid lines) to the data points for (A) ambient NO_3^- (k_{den} = 0.0046 m^{-1} or 16.4% of k_{tot}) and (B) NO_3^- addition experiments (k_{den} = 8.8 × 10^{-5} m^{-1} or 0.9% of k_{tot}). The dotted lines show the least-squares fits of the denitrification model to the tracer $^{15}N_2$ flux data using values of k_2 (N_2 gas exchange rate) approximately 0.5 and 2 times the measured k_2 values (k_2 of 0.03 and 0.11 m^{-1}, respectively). The dashed lines show the values of k_{den} that bound most of the data points for the average value of k_2 (0.055 m^{-1}). The upper dashed line in panel B represents the value of k_{den} needed to bound the bulb sample data point (open circle). *See Table 3* for a summary of k_{den} for each scenario.

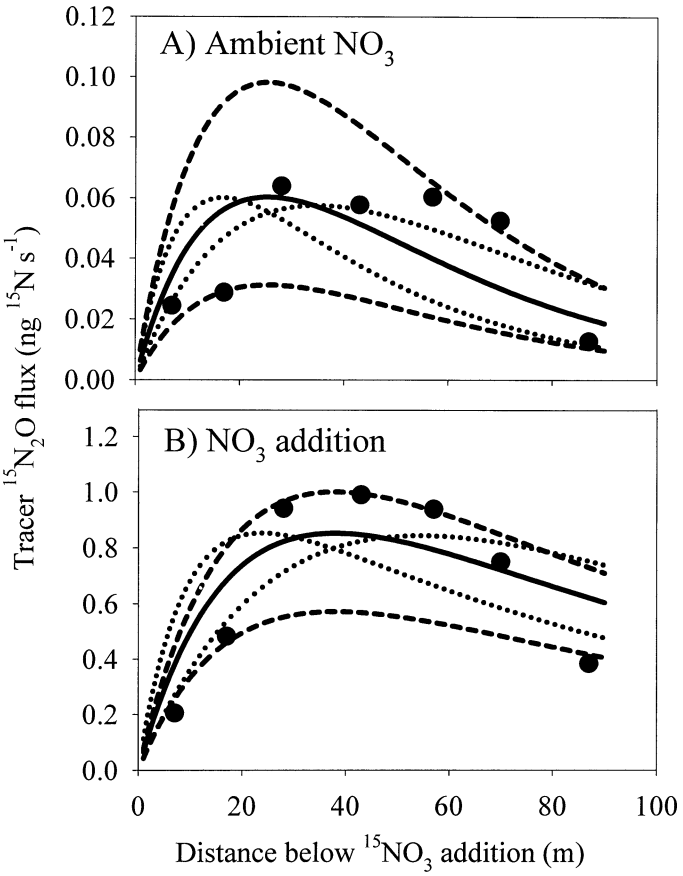

Fig. 6. Measured tracer $^{15}N_2O$ flux versus distance below the $^{15}NO_3^-$ addition (filled circles) and least-squares fits of the denitrification model (solid lines) to the data points for (A) ambient NO_3^- (k_{den} = 6.8 × 10^{-6} m^{-1} or 0.025% of k_{tot}) and (B) NO_3^- addition experiments (k_{den} = 3.0 × 10^{-6} m^{-1} or 0.03% of k_{tot}). The dotted lines show the least-squares fits of the denitrification model to the tracer $^{15}N_2O$ flux data using values of k_2 (N_2O gas exchange rate) approximately 0.5 and 2 times the measured k_2 value (k_2 of 0.03 and 0.11 m^{-1}). The dashed lines show the values of k_{den} that bound the data points for the average value of k_2 (0.054 m^{-1}). *See Table 3* for summary of k_{den} for each scenario.

to 57 m on an earlier date (13 June 2002) under similar stream discharge. Air–water exchange rates for N_2 and N_2O were therefore estimated to be 0.055 and 0.054 m^{-1}, respectively.

Denitrification rates (k_{den}) were determined by fitting the denitrification model to the tracer ^{15}N flux data for N_2 and N_2O production separately. The best-fit N_2 k_{den} was 0.0046 m^{-1} under ambient NO_3^- concentrations, representing about 16% of k_{tot} (Fig. 5A; Table 2). N_2 k_{den} declined to 8.8 × 10^{-5} m^{-1}, or about 1% of k_{tot} when NO_3^- concentration was increased on day 2 (Fig. 5B; Table 2). The mass flux rate of N_2 production per unit area (DN-N_2) was nearly threefold higher under ambient NO_3^- concentrations than under NO_3^- addition (Table 2). N_2O k_{den} values were considerably lower than N_2 k_{den} values, accounting for about 0.02% of k_{tot} under ambient NO_3^- concentrations (Fig. 6A; Table 2) and about 0.03% of k_{tot} when NO_3^- concentration was increased (Fig. 6B; Table 2). The mass flux rate of N_2O production per unit area (DN-N_2O) was about sixfold higher under NO_3^- addition than under ambient NO_3^- concentration (Table 2).

To provide an estimate of the impact of gas exchange rates on the uncertainty in the rates of k_{den} for N_2 and N_2O production, the denitrification model was fit to the data using values of the N_2 and N_2O gas exchange rates (k_2) one-half and two times the values of k_2 determined from the air–water exchange rates of propane. As a further analysis of uncertainty, we determined the values of k_{den} required to bound the majority of tracer $^{15}N_2$ and $^{15}N_2O$ flux data points for each experiment. These simulations are shown in Figs. 5 and 6, and the k_{den} values are summarized in Table 3. Based on this uncertainty analysis, k_{den} for N_2 production is constrained to range from 0.002 to 0.008 m^{-1} for the ambient NO_3^- experiment and from 3 to 21 × 10^{-5} m^{-1} for the NO_3^- addition experiment. Similarly, k_{den} for N_2O production is constrained

Table 3. Results of uncertainty analysis of denitrification rate (k_{den}) for N_2 and N_2O production for the ambient and NO_3^- addition experiments. Results are shown for the least-squares fit of the denitrification model to the tracer ^{15}N flux data using the air–water gas exchange rates (k_2) calculated from the mean gas exchange rate of propane. Results are also shown for two other scenarios to assess uncertainty: (1) the least-squares fit of the denitrification model to the tracer ^{15}N flux data using values of k_2 approximately one-half and 2 times the measured k_2 value and (2) the minimum and maximum k_{den} values necessary to bound the majority of the data points (*see Figs. 5 and 6*). The second maximum k_{den} value listed for N_2 production for the NO_3^- addition experiment is the model fit to the bulb sample (open data point in Fig. 5B).

Parameter	k_{den} (m^{-1})	
	Ambient	NO_3^- addition
N_2 production:		
Best model fit (k_2 = 0.055 m^{-1})	0.0046	8.8×10^{-5}
Uncertainty scenario 1:		
0.5 k_2 (0.03 m^{-1})	0.0031	5.5×10^{-5}
2 k_2 (0.11 m^{-1})	0.0075	15.7×10^{-5}
Uncertainty scenario 2:		
Minimum	0.0017	3×10^{-5}
Maximum	0.0080	16×10^{-5}
Maximum (bulb sample)	—	21×10^{-5}
N_2O production:		
Best model fit (k_2 = 0.054 m^{-1})	6.8×10^{-6}	3.0×10^{-6}
Uncertainty scenario 1:		
0.5 k_2 (0.03 m^{-1})	4.6×10^{-6}	1.9×10^{-6}
2 k_2 (0.11 m^{-1})	10.8×10^{-6}	5.3×10^{-6}
Uncertainty scenario 2:		
Minimum	3.5×10^{-6}	2.0×10^{-6}
Maximum	11.0×10^{-6}	3.5×10^{-6}

to range from 3.5 to 11 $\times$ 10^{-6} m^{-1} for the ambient NO_3^- experiment and from 1.9 to 5.3 $\times$ 10^{-6} m^{-1} for the NO_3^- addition experiment. For the ambient and NO_3^- addition experiments, respectively, the constrained ranges in N_2 production were 6.1% to 28.6% and 0.3% to 1.6% of k_{tot}. Similarly, N_2O production was 0.01% to 0.04% and 0.02% to 0.05% of k_{tot} for the ambient and NO_3^- addition experiments, respectively.

The uptake length of NO_3^- resulting from the total denitrification rate (sum of N_2 and N_2O production rates) was 217 m under ambient NO_3^- concentrations but increased to nearly 11 km when NO_3^- concentration was increased (Table 2). Based on the uncertainty analysis, the total denitrification-based NO_3^- uptake length is constrained to range from about 125 to 600 m for the ambient NO_3^- experiment and from about 5 to 32 km with NO_3^- addition.

Discussion

Total NO_3^- uptake rates—Total NO_3^- uptake rate per unit distance (k_{tot}) measured under ambient conditions in the East Fork of Walker Branch was among the highest and the NO_3^- uptake length (S_W) among the shortest values of these parameters reported for a number of small streams using the ^{15}N tracer addition approach (Peterson et al. 2001; Webster et al. 2003). The high k_{tot} and short S_W were primarily due to the low discharge, low average water velocity, and low water depth in the East Fork, which together enhance the contact time of stream water with sediments and biofilms where N uptake takes place. Total NO_3^- mass removal rate per unit area (U) and mass transfer velocity (V_f) in the East Fork under ambient NO_3^- concentrations were in the lower portion of the range reported for the streams in the Peterson et al. (2001) study, in part reflecting the low concentrations of NO_3^- characteristic of this stream.

Short-term (several hours) NO_3^- addition experiments also have been used to estimate NO_3 uptake lengths and rates in streams (e.g., Munn and Meyer 1990; Valett et al. 1996; Martí et al. 1997). Our value of S_W for the East Fork of Walker Branch under ambient NO_3^- was considerably shorter than values reported for other streams using the NO_3^- solute addition approach (generally 100 to >1,000 m). Although the relatively low discharge of the East Fork certainly accounts for some of these differences, methodological differences are also important. Mulholland et al. (2002) have shown that the nutrient addition approach results in overestimates of nutrient uptake length, with the magnitude of the overestimate a function of the degree of nutrient limitation and the magnitude of the nutrient addition. It may be possible to use a graphical extrapolation technique that involves extrapolation of uptake length–nutrient addition level relationships determined from nutrient addition experiments to obtain accurate estimates of uptake length, although this approach involves either multiple addition experiments under similar conditions or multiple sampling locations and the assumption of longitudinal homogeneity in stream conditions affecting nutrient uptake (Rob Payn and Jack Webster pers. comm.). Where feasible, however, the tracer addition approach such as used here with $^{15}NO_3^-$ is the most accurate and straightforward method for determining nutrient uptake length and uptake rate under ambient conditions in streams.

Denitrification rates—Our reach-scale, field ^{15}N addition and modeling approach indicated that the denitrification rate (expressed as a fractional NO_3^- removal rate, k_{den}) in the East Fork of Walker Branch under ambient NO_3^- concentrations was 0.0046 m^{-1}, with an uncertainty of about $\pm$0.003 m^{-1}. Thus, denitrification represented about 16% of the total NO_3^- removal rate from stream water under ambient conditions, with an uncertainty of about $\pm$10%. On a mass flux per unit area basis, the denitrification rate was 0.045 μg N m^{-2} s^{-1}, with an uncertainty of about $\pm$0.03 μg N m^{-2} s^{-1} under ambient NO_3^- concentrations. Denitrification consisted almost entirely of N_2 production (>99%), with very little N_2O production occurring.

Our uncertainty analysis included varying the air–water gas exchange rate (k_2) by a factor of 2 and determining the dentrification rates (k_{den}) necessary to bound most of the data points (Figs. 5 and 6). We believe that this analysis provides reasonable outer bounds on the uncertainty in the denitrification rate. The atmospheric N_2 contamination of our samples likely was the source of a considerable amount of the relatively high variability in the tracer $^{15}N_2$ flux data compared with the longitudinal pattern expected (Fig. 5). Sub-

sequent testing has implicated background N_2 in the exetainers prior to use as the likely source of most of the contamination (S. Hamilton unpubl. data). This might be avoided by reevacuating the exetainers and storing them under water prior to use. Nonetheless, our longitudinal ^{15}N data clearly indicate the presence of tracer ^{15}N in the dissolved N_2 and N_2O pools in stream water, and the longitudinal pattern showing a hump-shaped distribution of tracer ^{15}N flux in these pools is consistent with theoretical simulations using the denitrification model (Fig. 2).

The nearly sixfold increase in NO_3^- mass removal rate from water per unit area (U) with the approximately tenfold increase in NO_3^- concentration during the NO_3^- addition experiment appeared to be almost entirely the result of stimulation of assimilatory NO_3^- uptake. Denitrification rate expressed as a mass flux per unit area (DN) unexpectedly declined during the NO_3^- addition experiment relative to the ambient NO_3^- experiment (Table 2). A previous study using the C_2H_2 inhibition technique on Walker Branch sediments incubated in the laboratory suggested that denitrification was NO_3 limited (Martin et al. 2001). Consequently, we had expected to observe an increase in the mass flux denitrification rate with NO_3^- addition. The upper bound estimate of fractional denitrification rate for the NO_3^- addition experiment (21×10^{-5} m^{-1}; Table 3) translates to a mass flux denitrification rate that is about 70% of the ambient mass flux rate, so it is possible that the mass flux denitrification rate did not change much with NO_3^- addition. Regardless, our results suggest that denitrifiers were not capable of responding rapidly (within hours) to increases in streamwater NO_3^- in the field, as might occur during storms or other transient events, possibly due to carbon limitation or some other constraint. Carbon limitation may have been particularly strong at the time of this study because of low streamwater dissolved organic carbon concentrations (approximately 0.5 mg L^{-1}), low algal production rates (due to low light levels below the dense forest canopy), and low standing stocks of leaf detritus prior to the onset of autumn leaf fall.

The very low N_2O production rate relative to N_2 production rate in the East Fork of Walker Branch (N_2O/N_2 production ratios of 0.0015 and 0.032 for the ambient and NO_3^- addition experiments, respectively) are consistent with many previous studies of aquatic sediments. For example, in a survey of N_2O/N_2 production ratios reported for river, lake, and coastal marine sediments, Seitzinger (1988) reported that N_2O/N_2 production ratios were generally <0.05 and often <0.01. The ratios reported by Seitzinger also may be high when considering only denitrification because N_2O is also produced during nitrification and may account for some of the N_2O production in these studies. The relative proportions of N_2O and N_2 produced via denitrification are related to pH, oxygen, and H_2S concentrations, with higher N_2O production under more acid conditions or higher dissolved oxygen and H_2S concentrations (Seitzinger 1988). Recent work on soils suggests that the percentage water-filled pore space, which is proportional to the extent of anoxic conditions within the soil matrix, is a predictor of the N_2O/N_2 production ratio (Davidson et al. 2000). The pH of the East Fork of Walker Branch is approximately 7.5, and although dissolved oxygen concentrations of surface water are relatively high (approximately 8 mg L^{-1}), sediments and biofilms likely present great heterogeneity in redox conditions. Thus, in contrast to the relatively thorough anoxia typical of lake or ocean sediments, small streams could present a range of redox conditions, yet our results suggest that stream denitrification efficiently consumes nearly all of its N_2O intermediary.

The denitrification rate in the East Fork of Walker Branch (12 μmol N m^{-2} h^{-1}) was generally within the range of denitrification rates in other streams with NO_3^- concentrations <0.1 mg N L^{-1} (Table 4). Denitrification rates reported for streams and rivers with high NO_3^- concentrations (>1 mg N L^{-1}) are considerably greater (generally >100 μmol m^{-2} h^{-1}). Comparisons between the denitrification rate for the East Fork of Walker Branch and those reported for other streams and rivers are problematic, however, because of methodological differences and limitations. The rates reported using the C_2H_2 inhibition technique suffer from artifacts related to difficulties of adding C_2H_2 uniformly within sediments. The NO_3^- flux methods do not distinguish between denitrification and assimilatory NO_3^- uptake and may not account for nitrification. The C_2H_2, NO_3^- flux, and N_2 flux methods all require use of chambers or cores, which may reduce the exchange of surface water into and out of sediments. In addition, it can be problematic to extrapolate measurements made using chambers or cores to the entire stream ecosystem due to the complex spatial heterogeneity characteristic of most lotic ecosystems.

The field ^{15}N addition and modeling approach presented here does not suffer from the limitations described above and provides a reach-scale measure of denitrification in streams. However, this method does not include denitrification resulting from tightly coupled mineralization/nitrification/denitrification occurring entirely within sediments. Because we added tracer $^{15}NO_3^-$ only to the surface water and only for a short period, our approach includes only denitrification of NO_3^- that was originally in surface water or that exchanges rapidly with surface water NO_3^- pools. Thus, our method may underestimate total denitrification rate in stream ecosystems.

Seitzinger (1988), in her review of denitrification rates in aquatic ecosystems, reported that coupled mineralization/nitrification/denitrification in sediments comprised $>75\%$ of total denitrification in the Potomac and Delaware rivers, based on observations of high denitrification rates and low net NO_3^- flux into sediments. However, denitrification of streamwater NO_3^- may be more important in small streams with coarser sediments and more extensive and rapid mixing between surface and subsurface waters than in larger rivers characterized by fine-grained sediments with lower hydraulic conductivity. In a study of a small nitrate-rich stream in Denmark, Christensen et al. (1990) reported that the NO_3^- source for denitrification was primarily surface water NO_3^-, with minimal contribution from mineralization/nitrification in the sediments. In a study of denitrification in a small desert stream, Holmes et al. (1996) determined that denitrification rates were highest at downwelling areas where input of surface-derived organic matter and streamwater NO_3^- provided the substrates for denitrification in the sediments. Clearly, further research focusing on the coupling of mineralization,

Table 4. Denitrification rates measured in streams and rivers.

Stream/river, location	Watershed type	Denitrification rate (μmol m^{-2} h^{-1})	NO_3^- concentration (mg N L^{-1})	Method*	Reference
Salto River, Costa Rica	Lowland swamp forest	5–25	0.2	1	Duff et al. (1996)
		65–470	0.2	2	Duff et al. (1996)
Duffin Creek, Ontario	Forest and agriculture	10–125	5	3	Hill (1979)
Sycamore Creek, Arizona	Desert shrub	3–13	0.03	4	Holmes et al. (1996)
Kings Creek, Kansas	Prairie	0–9	0–0.03	5	Kemp and Dodds (2002)
San Francisquito Creek, California	Suburban	27	0.8–1	6	Duff et al. (1984)
Little Lost Man Creek, California	Forest	0	0.04	6	Duff et al. (1984)
Gelbaek, Denmark	Lowland, agriculture	100–1400	4–13	7	Christensen et al. (1990)
Rabis Baek, Denmark	Lowland	40–460	—	7	Christensen and Sorensen (1988)
Potomac River, Maryland	Mixed	210–232	>1	8	Seitzinger (1988)
Delaware River, New Jersey	Mixed	166–344	—	8	Seitzinger (1988)
Skit, New Jersey	Forest	<20	0.014	8	Seitzinger (1994)
Hammonton, New Jersey	Agriculture	250–450	1.8	8	Seitzinger (1994)
East Fork Walker Branch, Tennessee	Forest	12	0.03	9	This study
Sugar Creek, Indiana	Agriculture	120	0.9	9	Böhlke et al. 2004

* (1) C_2H_2 inhibition, benthic sediment chambers in field with C_2H_2 added to overlying water; (2) NO_3^- flux into sediments in benthic sediment chambers in field; (3) NO_3^- flux into sediment cores incubated in laboratory; (4) C_2H_2 inhibition, benthic sediment chambers with C_2H_2 added at sediment surface; (5) C_2H_2 inhibition, benthic communities (periphyton, filamentous algae, coarse and fine sediments, bryophytes) in flasks in lab at in situ temperatures; (6) C_2H_2 inhibition, periphyton communities on rocks incubated in chambers in laboratory with C_2H_2 added to overlying water; (8) N_2 flux, in intact sediment cores incubated in lab at in situ temperatures; (9) Field ^{15}N tracer addition ($^{15}NO_3^-$ addition to stream water).

nitrification, and denitrification and its contribution to total denitrification rate in streams is warranted.

The field ^{15}N addition approach has also been used to determine denitrification rates within an experimentally generated groundwater NO_3^- plume in a salt marsh (Tobias et al. 2001). The authors of this study estimated dentrification rates of about 1,000 μmol N m^{-2} h^{-1}, although they were unable to determine $^{15}N_2$ and $^{15}N_2O$ evasion rates because a conservative volatile tracer was not co-injected in the experiment.

A field ^{15}N addition approach quite similar to ours was recently used by Böhlke et al. (2004) to determine the denitrification rate in Sugar Creek, an agricultural stream in the upper Mississippi basin. The authors report a denitrification rate about an order of magnitude greater than that measured in Walker Branch, reflecting the 30-fold higher NO_3^- concentration in Sugar Creek (Table 4). Our study and that by Böhlke et al. demonstrate the usefulness of the field ^{15}N tracer addition approach for determining denitrification rates at the scale of entire stream reaches.

The field ^{15}N tracer addition approach may be impractical in streams and rivers with high discharge rates or high NO_3^- concentrations due to the cost of adding enough ^{15}N to achieve a sufficiently high ^{15}N enrichment of streamwater NO_3^-. We used a ^{15}N-NO_3^- enrichment of about 40,000‰, although considerably lower enrichment levels should be sufficient if denitrification rates are relatively high. For example, Böhlke et al. (2004) used a ^{15}N-NO_3^- enrichment about tenfold lower than we used in our study. The field ^{15}N tracer addition approach may also be problematic in high gradient streams with very high air–water gas exchange rates. Nonetheless, for many streams, our approach should be tractable and provides a reach-scale measure of the denitrification rate of NO_3^- in stream water as well as total NO_3^- uptake rate and length.

References

ALEXANDER, R. B., R. A. SMITH, AND G. E. SCHWARZ. 2000. Effect of stream channel size on the delivery of nitrogen to the Gulf of Mexico. Nature **403:** 758–761.

BÖHLKE, J. K., J. W. HARVEY, AND M. A. VOYTEK. 2004. Reach-scale isotope tracer experiment to quantify denitrification and related processes in a nitrate-rich stream, mid-continent USA. Limnol. Oceanogr. **49:** 821–838.

BOULTON, A. J., S. FINDLAY, P. MARMONIER, E. H. STANLEY, AND H. M. VALETT. 1998. The functional significance of the hyporheic zone in streams and rivers. Annu. Rev. Ecol. Syst. **29:** 59–81.

BOYER, E. W., C. L. GOODALE, N. A. JAWORSKI, AND R. W. HOWARTH. 2002. Anthropogenic nitrogen sources and relationships to riverine nitrogen export in the northeastern U.S.A. Biogeochemistry **57/58:** 137–169.

CHRISTENSEN, P. B., L. P. MIELSEN, J. SORENSEN, AND N. P. REVSBECH. 1990. Denitrification in nitrate-rich streams: Diurnal and seasonal variation related to benthic oxygen metabolism. Limnol Oceanogr. **35:** 640–651.

———, AND J. SORENSEN. 1988. Denitrification in sediment of lowland streams: Regional and seasonal variation in Gelbaek and Rabis Baek, Denmark. FEMS Microbiol. Ecol. **53:** 335–344.

DAVIDSON, E. A., M. KELLER, H. E. ERICKSON, L. V. VERCHOT, AND E. VELDKAMP. 2000. Testing a conceptual model of soil

emissions of nitrous and nitric oxides. BioScience **50:** 667–680.

DUFF, J. H., C. M. PRINGLE, AND F. J. TRISKA. 1996. Nitrate reduction in sediments of lowland tropical streams draining swamp forest in Costa Rica: An ecosystem perspective. Biogeochemistry **33:** 179–196.

———, F. J. TRISKA, AND R. S. OREMLAND. 1984. Denitrification associated with stream periphyton: Chamber estimates from undisrupted communities. J. Environ. Qual. **13:** 514–518.

GLASGOW, H. B., AND J. M. BURKHOLDER. 2000. Water quality trends and management implications from a five-year study of a eutrophic estuary. Ecol. Appl. **10:** 1024–1046.

HILL, A. R. 1979. Denitrification in the nitrogen budget of a river ecosystem. Nature **281:** 291–292.

HOLMES, R. M., J. B. JONES, JR., S. G. FISHER, AND N. B. GRIMM. 1996. Denitrification in a nitrogen-limited stream ecosystem. Biogeochemistry **33:** 125–146.

HOWARTH, R. W., AND OTHERS. 1996. Regional nitrogen budgets and riverine N and P fluxes for the drainages to the North Atlantic Ocean: Natural and human influences. Biogeochemistry **35:** 75–139.

INOUE, H. Y., AND W. G. MOOK. 1994. Equilibrium and kinetic nitrogen and oxygen isotope fractionations between dissolved and gaseous N_2O. Chem. Geol. (Isotope Geosci. Sect.) **113:** 135–148.

JÄHNE, B., G. HEINZ, AND W. DIETRICH. 1987. Measurement of the diffusion coefficients of sparingly soluble gases in water. J. Geophys. Res. **92:** 10767–10776.

JONES, J. B., AND P. J. MULHOLLAND. 2000. Streams and groundwaters. Academic.

JORDAN, T. E., AND D. E. WELLER. 1996. Human contributions to terrestrial nitrogen flux. BioScience **46:** 655–664.

KEMP, M. J., AND W. K. DODDS. 2002. The influence of ammonium, nitrate, and dissolved oxygen concentrations on uptake, nitrification, and denitrification rates associated with prairie stream substrata. Limnol. Oceanogr. **47:** 1380–1393.

KLOTS, C. E., AND B. B. BENSON. 1963. Isotope effect in the solution of oxygen and nitrogen in distilled water. J. Chem. Phys. **38:** 890–893.

MACINTYRE, S., R. WANNINKHOF, AND J. P. CHANTON. 1995. Trace gas exchange across the air-water interface in freshwater and coastal marine environments, pp. 52–97. *In* P. A. Matson and R. C. Harriss [eds.], Biogenic trace gases: Measuring emissions from soil and water. Methods in ecology. Blackwell.

MARTÍ, E., N. B. GRIMM, AND S. G. FISHER. 1997. Pre- and post-flood retention efficiency of nitrogen in a Sonoran Desert stream. J. N. Am. Benthol. Soc. **16:** 805–819.

MARTIN, L. A., P. J. MULHOLLAND, J. R. WEBSTER, AND H. M. VALETT. 2001. Denitrification potential in sediments of headwater streams in the southern Appalachian Mountains, U.S.A. J. N. Am. Benthol. Soc. **20:** 505–519.

MARZOLF, E. R., P. J. MULHOLLAND, AND A. D. STEINMAN. 1994. Improvements to the diurnal upstream-downstream dissolved oxygen change technique for determining whole-stream metabolism in small streams. Can. J. Fish. Aquat. Sci. **51:** 1591–1599.

MULHOLLAND, P. J. 1992. Regulation of nutrient concentrations in a temperate forest stream: Roles of upland, riparian, and instream processes. Limnol. Oceanogr. **37:** 1512–1526.

———, AND OTHERS. 2002. Can uptake length in streams be determined by nutrient addition experiments? Results from an inter-biome comparison study. J. N. Am. Benthol. Soc. **21:** 544–560.

MUNN, N. L., AND J. L. MEYER. 1990. Habitat-specific solute retention in two small streams: An intersite comparison. Ecology **71:** 2069–2082.

NEWBOLD, J. D., J. W. ELWOOD, R. V. O'NEILL, AND W. VAN WINKLE. 1981. Measuring nutrient spiraling in streams. Can. J. Fish. Aquat. Sci. **38:** 860–863.

NIELSEN, L. P. 1992. Denitrification in sediment determined from nitrogen isotope pairing. FEMS Microbiol. Ecol. **86:** 357–362.

NIXON, S. W., AND OTHERS. 1996. The fate of nitrogen and phosphorus at the land-sea margin of the North Atlantic Ocean. Biogeochemistry **35:** 141–180.

PETERSON, B. J., AND OTHERS. 2001. Control of nitrogen export from watersheds by headwater streams. Science **292:** 86–90.

RAINWATER, K. A., AND E. R. HOLLEY. 1984. Laboratory studies on hydrocarbon tracer gases. ASCE J. Environ. Eng. Div. **110:** 27–41.

RYSGAARD, S., N. RISGAARD-PETERSEN, L. P. NIELSEN, AND N. P. REVSBECH. 1993. Nitrification and denitrification in lake and estuarine sediments measured by the ^{15}N dilution technique and isotope pairing. Appl. Environ. Microbiol. **59:** 2093–2098.

SEITZINGER, S. P. 1988. Denitrification in freshwater and coastal marine ecosystems: Ecological and geochemical significance. Limnol. Oceanogr. **33:** 702–724.

———. 1994. Linkages between organic matter mineralization and denitrification in eight riparian wetlands. Biogeochemistry **25:** 19–39.

———, AND OTHERS. 2002. Nitrogen retention in rivers: Model development and application to watersheds in the northeastern U.S.A. Biogeochemistry **57/58:** 199–237.

SIGMAN, D. M., M. A. ALTABET, R. MICHENER, D. C. MCCORKLE, B. FRY, AND R. M. HOLMES. 1997. Natural abundance-level measurement of nitrogen isotopic composition of oceanic nitrate: an adaptation of the ammonium diffusion method. Marine Chemistry **57:** 227–242.

STREAM SOLUTE WORKSHOP. 1990. Concepts and methods for assessing solute dynamics in stream ecosystems. J. N. Am. Benthol. Soc. **9:** 95–119.

TOBIAS, C. R., S. A. MACKO, I. C. ANDERSON, E. A. CANUEL, AND J. W. HARVEY. 2001. Tracking the fate of a high concentration groundwater nitrate plume through a fringing marsh: A combined groundwater tracer and in situ isotope enrichment study. Limnol. Oceanogr. **46:** 1977–1989.

TURNER, R. E., AND N. N. RABALAIS. 1994. Coastal eutrophication near the Mississippi river delta. Nature **368:** 619–621.

VALETT, H. M., J. A. MORRICE, C. N. DAHM, AND M. E. CAMPANA. 1996. Parent lithology, surface-groundwater exchange, and nitrate retention in headwater streams. Limnol. Oceanogr. **41:** 333–345.

VITOUSEK, P. M., AND OTHERS. 1997. Human alteration of the global nitrogen cycle: Sources and consequences. Ecol. Appl. **7:** 737–750.

WANNINKHOF, R. 1992. Relationship between wind speed and gas exchange over the ocean. J. Geophys. Res. **97:** 7373–7382.

———, P. J. MULHOLLAND, AND J. W. ELWOOD. 1990. Gas exchange rates for a first-order stream determined with deliberate and natural tracers. Water Resour. Res. **26:** 1621–1630.

WEBSTER, J. R., AND OTHERS. 2003. Factors comparing ammonium uptake in streams—an interbiome perspective. Freshwater Biol. **48:** 1329–1352.

WISE, D. L., AND G. HOUGHTON. 1966. The diffusion coefficients of ten slightly soluble gases in water at 10–60 deg C. Chem. Eng. Sci. **21:** 999–1010.

Received: 23 May 2003
Accepted: 8 October 2003
Amended: 12 December 2003